AGU PUBLICATIONS

JGR

Journal of Geophysical Research: Space Physics

RESEARCH ARTICLE
10.1002/2015JA021023

Key Points:
- Westward moving brightenings near the auroral equatorward boundary are common and are associated with azimuthally moving flow bursts near or within SAPS region
- Azimuthal flow bursts connect to earthward plasma sheet flow bursts

Supporting Information:
- Movies S1–S5
- Movie S1
- Movie S2
- Movie S3
- Movie S4
- Movie S5

Correspondence to:
L. R. Lyons,
larry@atmos.ucla.edu

Citation:
Lyons, L. R., et al. (2015), Azimuthal flow bursts in the inner plasma sheet and possible connection with SAPS and plasma sheet earthward flow bursts, *J. Geophys. Res. Space Physics*, *120*, 5009–5021, doi:10.1002/2015JA021023.

Received 16 JAN 2015
Accepted 8 MAY 2015
Accepted article online 11 MAY 2015
Published online 5 JUN 2015

Azimuthal flow bursts in the inner plasma sheet and possible connection with SAPS and plasma sheet earthward flow bursts

L. R. Lyons[1], Y. Nishimura[1], B. Gallardo-Lacourt[1], M. J. Nicolls[2,3], S. Chen[2,3], D. L. Hampton[4], W. A. Bristow[4], J. M. Ruohoniemi[5], N. Nishitani[6], E. F. Donovan[7], and V. Angelopoulos[8]

[1]Department of Atmospheric and Oceanic Sciences, University of California, Los Angeles, California, USA, [2]Center for Geospace Studies, SRI International, Menlo Park, California, USA, [3]Space Sciences Laboratory, University of California, Berkeley, California, USA, [4]Geophysical Institute, University of Alaska Fairbanks, Fairbanks, Alaska, USA, [5]Bradley Department of Electrical and Computer Engineering, Virginia Tech, Blacksburg, Virginia, USA, [6]Solar-Terrestrial Environment Laboratory, Nagoya University, Nagoya, Japan, [7]Department of Physics and Astronomy, University of Calgary, Calgary, Alberta, Canada, [8]Department of Earth, Planetary, and Space Sciences, University of California, Los Angeles, California, USA

Abstract We have combined radar observations and auroral images obtained during the Poker Flat Incoherent Scatter Radar Ion Neutral Observations in the Thermosphere campaign to show the common occurrence of westward moving, localized auroral brightenings near the auroral equatorward boundary and to show their association with azimuthally moving flow bursts near or within the subauroral polarization stream (SAPS) region. These results indicate that the SAPS region, rather than consisting of relatively stable proton precipitation and westward flows, can have rapidly varying flows, with speeds varying from ~100 m/s to ~1 km/s in just a few minutes. The auroral brightenings are associated with bursts of weak electron precipitation that move westward with the westward flow bursts and extend into the SAPS region. Additionally, our observations show evidence that the azimuthally moving flow bursts often connect to earthward (equatorward in the ionosphere) plasma sheet flow bursts. This indicates that rather than stopping or bouncing, some flow bursts turn azimuthally after reaching the inner plasma sheet and lead to the bursts of strong azimuthal flow. Evidence is also seen for a general guiding of the flow bursts by the large-scale convection pattern, flow bursts within the duskside convection being azimuthally turned to the west, and those within the dawn cell being turned toward the east. The possibility that the SAPS region flow structures considered here may be connected to localized flow enhancements from the polar cap that cross the nightside auroral poleward boundary and lead to flow bursts within the plasma sheet warrants further consideration.

1. Introduction

Large-scale convection describes transport along plasma sheet magnetic fields well over large spatial and long temporal scales. However, localized bursts (−few R_E across) of strongly enhanced earthward flow make a major contribution to transport within the plasma sheet [*Angelopoulos et al.*, 1992, 1997] and map along magnetic field lines where they are seen in the ionosphere as bursts or channels of enhanced equatorward flow [*Sergeev et al.*, 1990; *Yeoman and Lühr*, 1999; *Kauristie et al.*, 1996]. Such bursts of equatorward flow typically occur within a few hours of magnetic midnight and are associated with auroral intensifications along the poleward boundary of the auroral oval (poleward boundary intensifications, or PBIs) [*de la Beaujardière et al.*, 1994; *Lyons et al.*, 1999; *Zesta et al.*, 2000]. PBIs can extend equatorward from the poleward boundary of the auroral oval in association with plasma sheet flow bursts [*Nakamura et al.*, 1993; *Rostoker et al.*, 1987; *Henderson et al.*, 1998; *Sergeev et al.*, 2000; *Zesta et al.*, 2000, 2002], the aurora structures crossing latitude lines unlike east-west auroral arcs. Such structures are now generally referred to as auroral streamers. Flow bursts are seen in the ionosphere are aligned with and adjacent to essentially all streamers [*Gallardo-Lacourt et al.*, 2014], and these flow bursts can be seen simultaneously in the ionosphere and in the plasma sheet [*Pitkänen et al.*, 2011]. Thus, in addition to magnetospheric and ionospheric flow measurements, auroral streamers can be used to identify plasma sheet flow bursts and their earthward extension as mapped to the ionosphere.

Auroral streamers can extent to near the equatorward boundary of the auroral oval, implying that plasma sheet flow bursts can move earthward from the deep tail to the near-Earth portion of the plasma sheet. Some flow bursts even move earthward of field lines threading the auroral oval, as evidenced by storm

main phase observations of streamers leading to subauroral proton auroral brightenings [*Nishimura et al.*, 2014b] and of bursty ion injection into the partial ring current [*Gkioulidou et al.*, 2014]. Flow bursts have often been treated as moving earthward and stopping within the plasma sheet, as has been seen in the MHD simulations of *Birn and Hesse* [2013] and *Birn et al.* [2013]. There is also a proposal that flow bursts oscillate back and forth in radial distance as they stop within the near-Earth plasma sheet [*Wolf et al.*, 2012], and this proposal has been supported by oscillatory flows observed in the plasma sheet by *Panov et al.* [2013, 2014].

However, there have been a few case studies where aurora and radar flow observations have been used together and have yielded evidence that some flow bursts, rather than stopping, can turn azimuthally after reaching the inner plasma sheet [*Kauristie et al.*, 2003], yielding bursts of strong azimuthal flow having a direction controlled by the large-scale convection pattern [*Zou et al.*, 2009a]. *Makarevich et al.* [2011] presented an example where a flow burst turned westward after reaching the subauroral polarization stream (SAPS) region, forming a latitudinally narrow burst of strongly enhanced flow within the region that lies equatorward of the electron auroral oval. SAPS are strong westward flows within the duskside convection cell. They result from the closing of the downward Region 2 currents that are formed at afternoon-to-midnight magnetic local times (MLTs) by plasma sheet protons that drift earthward of the field lines of the electron auroral oval and comprise the partial ring current. Localized bursts of enhanced flow within the larger-scale westward flows of the SAPS region have been observed and are often referred to as subauroral ion drifts (SAIDs) [*Foster and Burke*, 2002; *Spiro et al.*, 1979]. The magnitude of the SAID flow increases can be larger than that of the background SAPS flow [e.g., *Mishin and Burke*, 2005], so that azimuthal turning of plasma sheet flow bursts has the possibility of making a significant contribution to SAPS flow dynamics. Furthermore, a connection of SAID flow enhancements to plasma sheet flow bursts is suggested by an observed association with plasma sheet injection features [*Mishin*, 2013].

Here we combine radar observations and auroral images to show the existence of westward moving, localized auroral brightenings near the auroral equatorward boundary and to show that they are associated with azimuthally moving flow bursts near or within the SAPS region. We also show that there is a possible connection to the earthward moving plasma sheet flow bursts that are manifested as auroral streamers. We use data from the Poker Flat Incoherent Scatter Radar (PFISR) Ion Neutral Observations in the Thermosphere campaign, a multiground-based instrumentation campaign to measure auroral ionosphere and thermosphere that was designed around the Advanced Modular Incoherent Scatter Radar in Poker Flat, Alaska (PFISR), where magnetic midnight is at ~11:00 UT. The campaign dates of interest are 5–25 November 2012 and 6–22 March 2013, from which there were 29 nights with at least 1 h of clear skies and simultaneous PFISR measurements. We primarily use data from PFISR and the multispectral all-sky imager (ASI) at Poker Flat. For two events, we are able to take advantage of the larger spatial coverage offered by neighboring Time History of Events and Macroscale Interactions during Substorms (THEMIS) white-light ASIs [*Donovan et al.*, 2006] and Super Dual Auroral Radar Network (SuperDARN) radars.

2. Westward Moving Auroral Enhancements and Associated Flow Bursts

Figure 1 shows times series of two westward moving forms near the equatorward boundary of the auroral oval on 23 March 2012. Here line of sight (LOS) flows from PFISR are overlaid on images in geomagnetic coordinates of auroral 557.7 nm (green line) emissions taken by the ASI at Poker Flat. The intensity scale has been adjusted to show the relatively weak azimuthally moving auroral forms identified by a red arrow in each image, although this intensity scale leads to saturation of some of the brighter auroral features within the poleward potion of the oval. Movie S1 in the supporting information shows the auroral images observations every 13 s from 07:00 to 08:40 UT, together with the radar flows analyzed with similar time resolution. The movie clearly shows that the forms identified in Figure 1 were two of several forms that swept from east to west during this period within the equatorward portion of the auroral oval. Our observations indicate that azimuthally moving auroral forms such as seen in Figure 1 and Movie S1 in the supporting information are quite common, being seen during premidnight MLT time intervals on 24 of the 29 nights of observations.

Since these auroral forms are moving westward, they are likely associated with westward flows. Also, auroral enhancements are expected to reflect enhancements in upward field-aligned currents that connect with an adjacent enhancement in electric field-driven currents in the ionosphere. Thus, under the assumption of

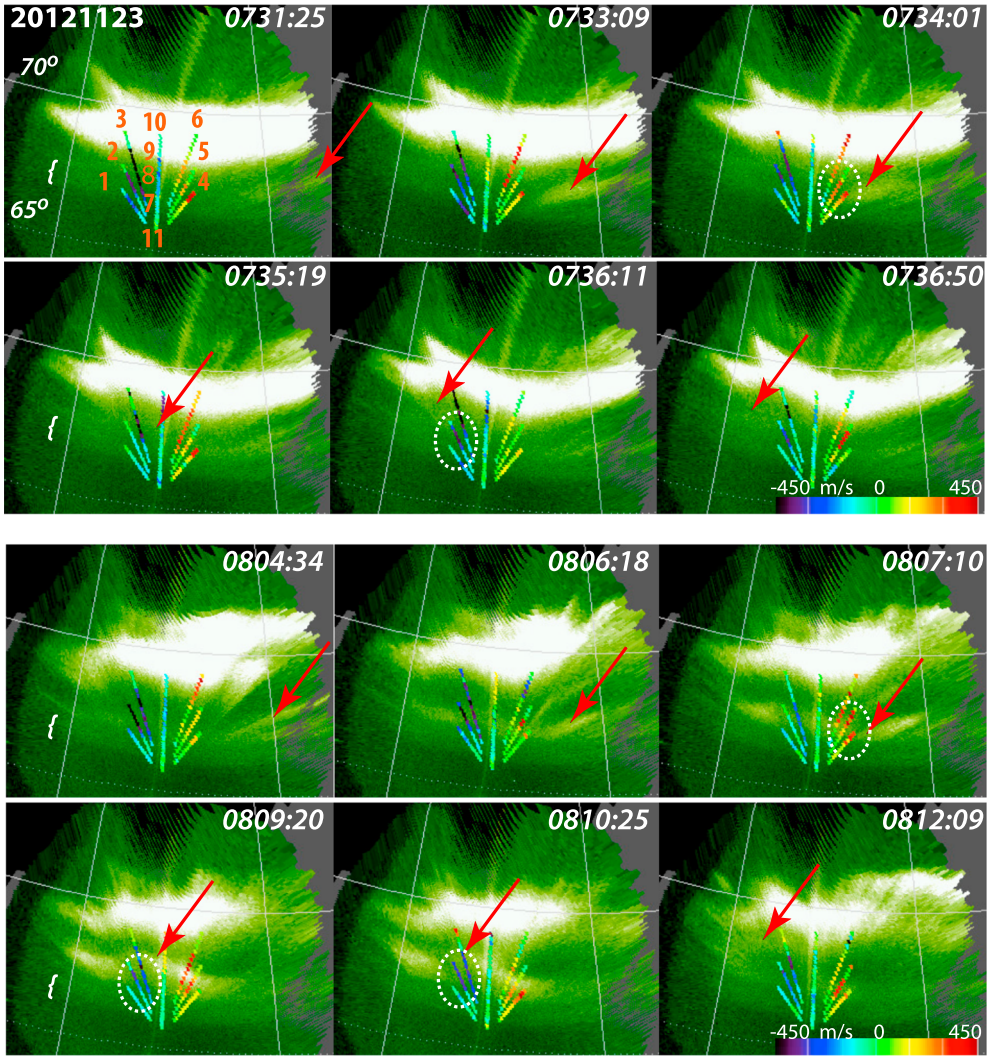

Figure 1. Times series of two westward moving forms near the equatorward boundary of the auroral oval on 23 March 2012. PFISR LOS flows are overlaid on images in geomagnetic coordinates of 557.7 nm from the Poker Flat ASI. The auroral intensity scale has been adjusted to show the relatively weak azimuthally moving forms identified by a red arrow in each image. PFISR beam numbers are identified in the top left plot. The dashed white ellipses for each case identify regions where the LOS flows show a speed enhancement first seen in the eastward looking beams and then in the westward looking beams. LOS speeds are color coded, with positive being toward the radar. The white bracket in the images along the left edge identifies the equatorward diffuse auroral band attributable to proton precipitation.

westward flow, current continuity indicates that the electric field enhancement would be a westward moving enhancement in northward electric fields lying just equatorward of the auroral enhancements. The particular events on this day were chosen because the auroral enhancements moved across the field of view (FOV) of PFISR, allowing measurement of ionospheric flows relative to the auroral enhancements. The PFISR operating mode on this day had three beams looking toward the east with different azimuthal angles, three similarly to the west, four to the north with different elevation angles, and one looking up the local magnetic field *B* direction. The colored dots overlaid on the images give LOS flows along all but the up *B* beam, and the corresponding beam numbers are labeled in the first panel.

In Figure 1, the LOS flow measurements equatorward of the more poleward, brighter aurora are toward the radar in the eastward looking beams, away from the radar in the westward looking beams, and weak in

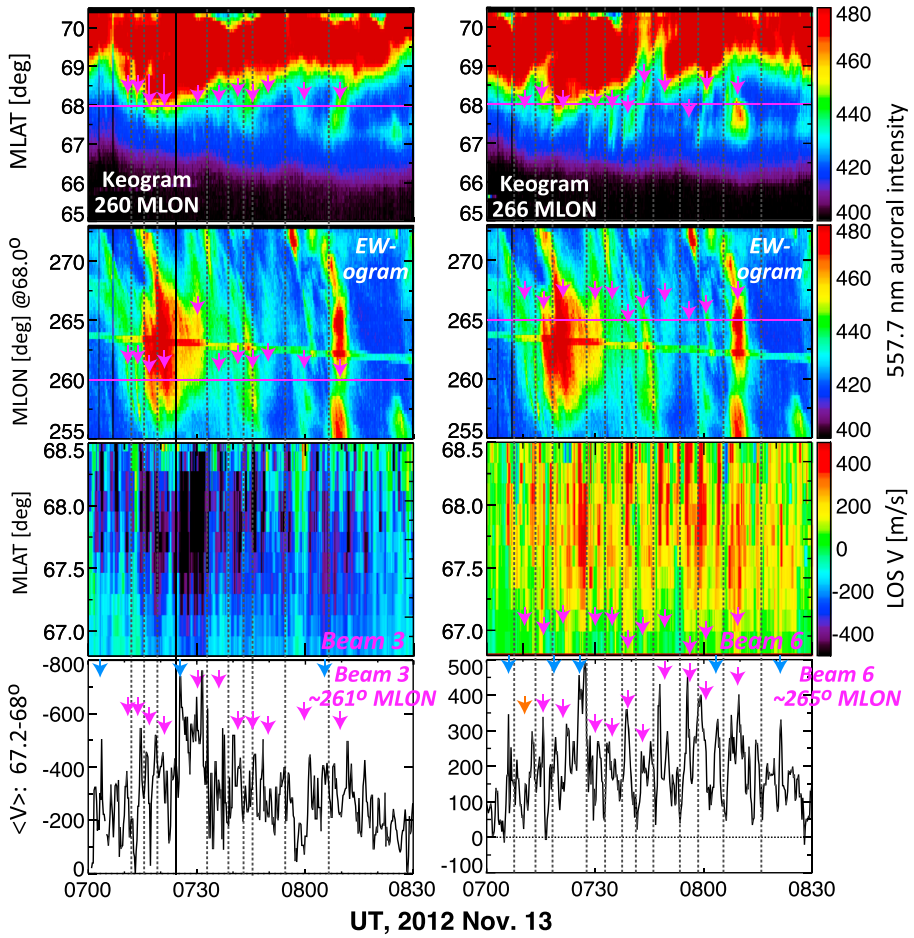

Figure 2. (first row) Keograms of auroral intensities on 23 March 2012 along longitudes to the west of (left column) and to the east of (right column) Poker Flat. (second row) Auroral intensity as a function of MLON at 68° MLAT. The horizontal magenta line marks the MLON where the PFISR radar beams 3 (left column) and 6 (right column) cross 68° MLAT, these being the longitudes of the keograms in the first row. (third row) LOS speeds as a function of MLAT along beam 3 (left column) and beam 6 (right column). (fourth row) LOS speeds averaged from 67.2° to 68° MLAT. The downward pointing magenta arrows in the first and second rows give the times at which each identifiable auroral enhancement crosses the radar beam at 68° MLAT (vertical placement chosen for visual clarity). The vertical black dotted lines are drawn to visually separate the different azimuthally moving enhancements. The magenta arrows overlaid on the bottom plot (and the third row on the right column) are at the same times as in the first and second rows. The auroral arrow drawn in orange does not point (within ~1–2 min) to a peak in the averaged LOS speeds in the fourth row. The blue arrows identify bursts of enhanced flow that we were unable to associate with a detectable auroral enhancement.

poleward looking beams. This is the typical signature of westward flow extending across the PFISR FOV. The dashed white ellipses identify regions where the LOS flows show an enhancement that is first seen in the eastward looking beams and then in the westward looking beams as consistent with a westward moving enhancement in the westward flows moving across the radar beams. Note that the LOS flow enhancements are quite large, reaching magnitudes >400 m/s. This implies that the actual magnitude of the westward flow enhancements was several hundred meters per second higher, due to the substantial angle between the radar beam look directions and the azimuthal direction.

Figure 2 shows the ASI and radar LOS flow data in a format chosen to test for an overall association between the azimuthally moving auroral forms and large enhancements in the westward flows, which, as we will demonstrate, extend equatorward to the SAPS region. The top two plots show keograms of the auroral intensities along longitudes to the west of (left side) and to the east of (right side) Poker Flat. With the intensity scale chosen, the more poleward auroral intensities are again saturated. However, the weaker auroral enhancement can be seen extending roughly from 66.5° to 68.5° magnetic latitude (MLAT), leading

to a very irregular equatorward boundary of electron precipitation as a function of time. The second panels then show the auroral intensity as a function of magnetic longitude (MLON) at 68° MLAT (referred as an ewogram for "east-west-o-gram" [*Donovan et al.*, 2006]). This latitude was chosen because, as can be seen from the horizontal magenta line in the top plots, essentially all of the weak, equatorward auroral enhancements extend across this latitude. The clear tilt of the auroral enhancement features shows that the enhancements are moving across the ewograms from east to west. In these panels, a horizontal magenta line marks the MLON where the PFISR radar beams 3 (left side) and 6 (right side) crosses 68° MLAT. These are the same longitudes of the keograms in the top plots. Downward pointing magenta arrows in the second panels give the times at which each identifiable auroral enhancement crosses the radar beam at 68° MLAT (their vertical placement being chosen for visual clarity). Also for clarity, the vertical black dotted lines are drawn to visually separate the different azimuthally moving enhancements.

Radar LOS speeds are shown in the bottom two plots. The third panels show the LOS speeds as a function of MLAT along beam 3 (left) and beam 6 (right). It is immediately apparent that the westward flow speed in this region varied strongly within a few minutes so as to give LOS speeds from close to 0 to $>$400 m/s, and that this variability extends over the ~1.75° range of MLAT shown. To provide a quantitative measure, the bottom plots of Figure 2 show the LOS speeds averaged from 67.2° to 68° MLAT, which is just equatorward of the auroral intensities show in the ewograms. The large variability of the flows shows clearly, even in the averages. The peaks in the average LOS flows are typically ~500 km/s, so that the full westward flow speeds likely reach close to 1 km/s.

Overlaid on the bottom plots (and the third panel on the right side) in Figure 2 are magenta arrows placed at the same times as in the second panel. All of these arrows (except for the one drawn with an orange color) can be seen to point (within ~1–2 min) to a peak in the averaged LOS speeds in the bottom plots, indicating that almost all the azimuthally moving auroral enhancements were associated with a burst of enhanced westward flow. The reverse is not true, however, since there are few identifiable bursts of enhanced flow (downward pointing blue arrows) that we were unable to associate with a detectable auroral enhancement.

The next question we address using this event is whether the westward directed flow bursts are able to penetrate sufficiently equatorward so as to reach the SAPS region. To identify the SAPS region, we look at auroral emissions and corresponding *E* region ionization that indicate the presence of precipitation of protons from the partial ring current in the region equatorward of most of the electron aurora. Protons undergo multiple charge exchange interactions as they precipitate, causing proton precipitation to smoothly spread over ~1–2° in latitude. Moreover, proton precipitation leads to auroral green line emissions due to secondary electrons produced by proton precipitation (see review by *Donovan et al.* [2012]), so that proton auroral emissions can be seen in the ASI images used here. On the evening side, the proton aurora typically forms a band of diffuse aurora adjacent to the equatorward boundary of the electron auroral oval [*Donovan et al.*, 2012; *Eather and Mende*, 1972; *Mende and Eather*, 1975; *Zou et al.*, 2012]. Such a diffuse band can be seen extending from east to west as the equatorward most discernible auroral emissions in Figure 1 (where the band is identified by a white bracket in the images along the left edge) and in Movie S1 in the supporting information. The westward moving auroral enhancements appear to sweep adjacent to, or within the poleward portion, of this diffuse band, consistent with them being within or adjacent to the region of SAPS.

To test whether the equatorward diffuse emission band indeed does result from proton precipitation, we use the PFISR radar measurements of electron density. Proton precipitation has been found [*Lilensten and Galand*, 1999; *Smirnova et al.*, 2004] to give a prominent ionization peak in the *E* region ($<$150 km) that decreases significantly below ~100 km, and this peak has been validated with spacecraft particle observations [*Zou et al.*, 2009b]. Figure 3 (left) shows electron densities measure by PFISR along the three most poleward looking of the central meridian beams from 07:00 to 08:30 UT, which includes the times of the images in Figure 1. Measurement altitude and MLAT are indicated along the vertical axes. Densities below 150 km are shown from the alternating code transmission scheme, which gives ~5 km resolution in the *E* region and can thus identify the ionization peak due to proton precipitation. Densities above 150 km are shown from the long pulse mode, which gives ~25 km resolution extending up in to the *F* region. Noise increases as the square of distance from the radar, becoming significant in the alternating code densities close to 150 km, and this causes the apparent discontinuity between the two modes at 150 km.

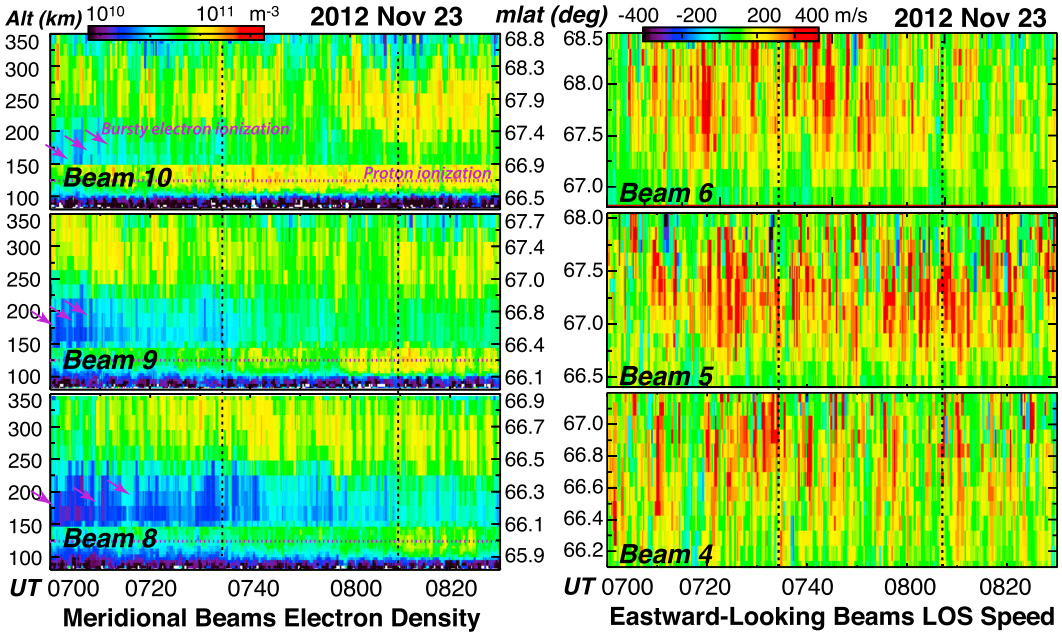

Figure 3. (left column) Electron densities measured by PFISR along the three most poleward looking of the central meridian beams from 07:00 to 08:30 UT on 13 March 2012, which includes the times of the images in Figure 1. Densities below 150 km are shown from the alternating code transmission scheme, and densities above 150 km are shown from the long pulse. Noise increases as the square of distance from the radar, becoming significant in the alternating code densities close to 150 km. The dotted horizontal lines are drawn at 125 km to assist in identifying the ionization layer from proton precipitation. The magenta arrows identify the first three clear bursts of electron precipitation ionization seen by each beam. (right column) LOS flow speeds along the three eastward looking PFISR beams. Note that latitudes for the left column are given along their right vertical axes and for the right column along their left vertical axes. The dashed vertical lines in the left (right) column give the times that the two auroral enhancements (flow bursts) used for illustration in Figure 1 crossed the meridional (eastward looking) radar beams.

In Figure 3, an *E* region layer of enhanced densities can be seen extending from ~115 to ~140 km altitude, and this layer is generally distinct from the bursty enhancements in ionization that extend down from ~225 km and are due to electron precipitation. The *E* region layer is the layer expected from proton precipitation. Its ionization increase with altitude below the peak is very clear. A decrease in ionization above the peak is generally also discernible but is affected by the increase in noise at ~140–150 km. The layer can be seen in beams 9 and 10 throughout the time interval shown. It appeared also in beam 8, particularly after ~07:35 UT, but is considerably weaker than in beams 9 and 10. This indicates that a proton precipitation region extended from ~66° to above 66.7° MLAT, this being approximately consistent with the diffuse auroral region in the ASI images that we have interpreted as the SAPS region.

Figure 3 (right) shows the LOS flow speeds from the three eastward looking PFISR beams, and the bursty flow enhancements can be seen to have extended equatorward to 66° MLAT and clearly well into the latitude range of the proton precipitation ionization. The times that the two bursts in Figure 1 crossed the eastward looking beams are identified by dashed vertical lines, and these bursts can be seen in the LOS flows extending over ~1–2° in latitude. Furthermore, occasional bursts of ionization from electron precipitation are clearly seen in beams 9 and 10 within the latitude range of the proton precipitation (and are seen more persistently at the higher latitudes of beam 10). The magenta arrows in Figure 3 (left) identify the first three clear bursts of electron precipitation ionization seen by each beam. The times that the two auroral enhancements used for illustration in Figure 1 crossed the meridional radar beams are identified by dashed vertical lines in Figure 3 (left), and the corresponding bursts of ionization can be seen in beam 8 at ~66.2–66.4° MLAT. Note that the duration of the ionization bursts is generally about the same of that of the flow bursts in the left-hand plots.

It is interesting, however, that the bursty enhancements of ionization extending down from higher altitude penetrate into the region of the proton precipitation region. This indicates that while dominated by

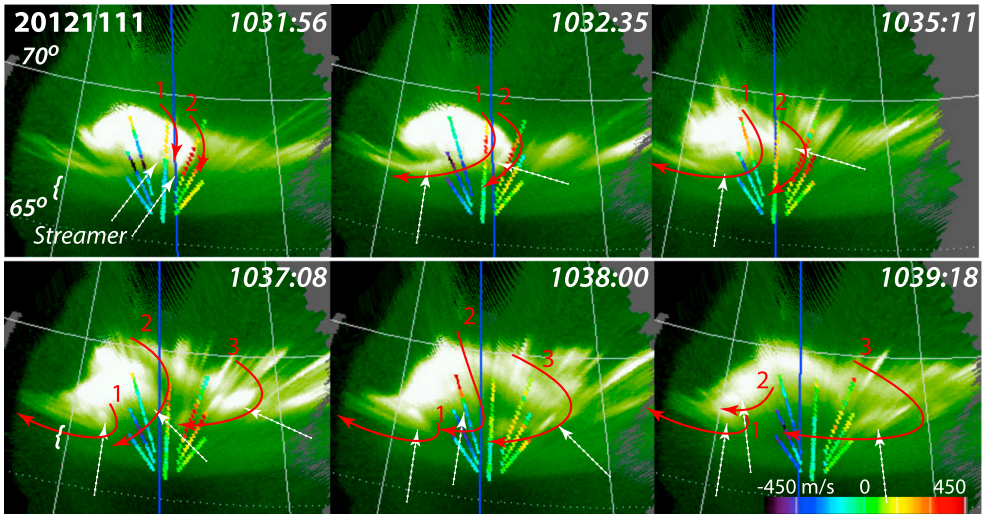

Figure 4. Time series of LOS flows from PFISR overlaid on green line images from the multispectral ASI at Poker Flat on 11 November 2012. The curved red arrows illustrate the ionospheric paths of the plasma sheet flow bursts estimated using paths of the auroral streamers and the LOS flows observed by PFISR. The dashed white arrows identify streamers used for estimating these paths. The white bracket in the images along the left edge identifies the equatorward diffuse auroral band attributable to proton precipitation.

proton precipitation, bursts of weak electron precipitation can at times penetrate into portions of the SAPS region. These observations indicate that the SAPS region should not be viewed as a region of relatively stable proton precipitation and westward flows but instead can include strong westward flow bursts and associated weak bursts of electron precipitation.

3. Connection to Earthward Plasma Sheet Flow Bursts

The above example shows that westward moving, localized auroral brightenings near the auroral equatorward boundary, which we have found to be common during our periods of observations, are associated with azimuthally moving flow bursts near or within the SAPS region. We next show examples to show the possible connection of the azimuthal flow bursts to plasma sheet flow bursts, which are manifested as auroral streamers. Figure 4 shows a time series of LOS flows from PFISR overlaid on green line images from the multispectral ASI at Poker Flat on 11 November 2012. The intensity scale has been adjusted to show the aurora streamers that extended equatorward from near the auroral poleward boundary, within a region of bright auroral having a surge-like shape, and then turned azimuthally near the auroral equatorward boundary and becoming weak azimuthally moving auroral enhancements. Movie S2 in the supporting information shows the auroral images for this time period every 13 s from 10:25 to 10:55 UT, together with the radar flows analyzed with similar time resolution. (Note that auroral streaks appearing to converge toward the zenith are auroral rays extending upward along magnetic field lines.)

The curved red arrows in Figure 4 illustrate the ionospheric paths of the plasma sheet flow bursts qualitatively estimated by assuming that flows lie adjacent and parallel to auroral streamers, with the additional requirement of consistency with the LOS flows observed by PFISR. The streamers used for estimating these paths are identified by dashed white arrows, their identification as streamers generally showing more clearly when viewing the movie than in the individual images. These paths indicate that the westward moving flow bursts arise from equatorward moving (earthward moving in the plasma sheet) flow bursts. Such a connection is apparent from the shape and paths of the streamers, and it is also supported by the PFISR observations showing both equatorward flow enhancements associated with the more poleward equatorward oriented portions of the streamers and enhancements consistent with westward flows associated with the azimuthally oriented portion of the streamers. The inferred flow bursts appear to be guided by the large-scale background flow, flowing equatorward and around the Harang reversal, and then flowing westward within the region what appears to be the proton aurora within the SAPS region.

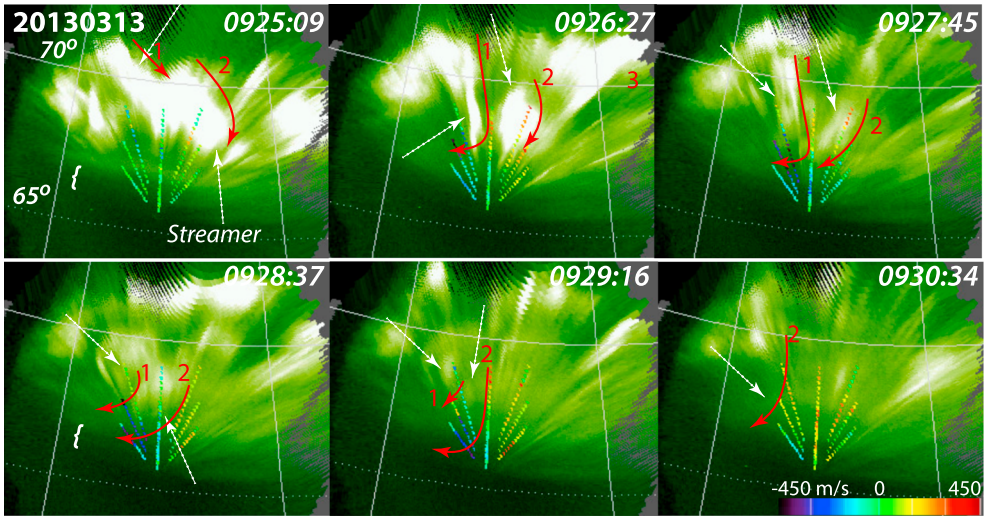

Figure 5. Time series of LOS flows from PFISR overlaid on green line images from the multispectral ASI at Poker Flat on 13 March 2013 in the same format as Figure 4.

Movie S2 in the supporting information shows evidence that some of the flows reached the equatorward auroral band that we attribute to proton precipitation observations.

A second example (on 13 March 2013) is shown in Figure 5 and Movie S3 in the supporting information, where the curved red arrows in the figure again illustrate the flow burst paths as inferred from the observations. This example shows further evidence that equatorward moving flow bursts turn westward, becoming the westward moving flow bursts that give the westward moving aurora enhancements. This example was selected because it shows more clearly that the flow bursts reached the equatorward diffuse auroral band that we attribute to proton precipitation observations and then turned westward.

For further verification that the diffuse equatorward band is the proton precipitation region of SAPS region, Figure 6 shows electron densities measured by PFISR along all the central meridian beams, as well as along the up *B* beam, from 10:15 to 11:15 UT on 11 November 2012 and from 09:00 to 09:45 UT on 13 March 2013, which include the times of the images in Figures 4 and 5. For the 11 November 2012 period, the proton ionization layer well separated from the higher-altitude ionization can be seen continuously from ~67° down to the latitude, 65.4°, of the up *B* radar beam 11; this being approximately consistent with the equatorward auroral band in Figure 4 that we attribute to proton precipitation. Bursts of electron aurora ionization that extend down from ~225 km are also seen, although the radar data have been processed for this event at 1 min time resolution making the short-time scales structure less clear than in Figure 3. The proton ionization layer is also clearly seen, and over a similar latitude region, for the 13 March 2013 period. Intrusions of weak electron auroral ionization are most intense during the time interval ~09:25–09:35 UT, which corresponds to the time of the equatorwardmost flow bursts inferred from the auroral images and seen by PFISR. This implies that as for the above event, the flows extended into the SAPS, as can be seen in Figure 5 and Movie S2 in the supporting information, and that the SAPS region included strong westward flow bursts and associated weak electron precipitation bursts.

An azimuthal turning of streamers leading to azimuthal moving auroral forms at premidnight to midnight MLTs, such as seen in the above examples, was seen during 18 of the 29 nights of our observations. It is likely that this connection is even more common than this, since this was seen using only one ASI and connections to the east of the ASI FOV will lead to azimuthal auroral enhancements that are seen within the FOV.

4. Broader Coverage Events

For two of our events, we have good coverage from both neighboring THEMIS white-light ASIs and SuperDARN coherent-scatter radars, offering broader spatial converge than can be obtained with the

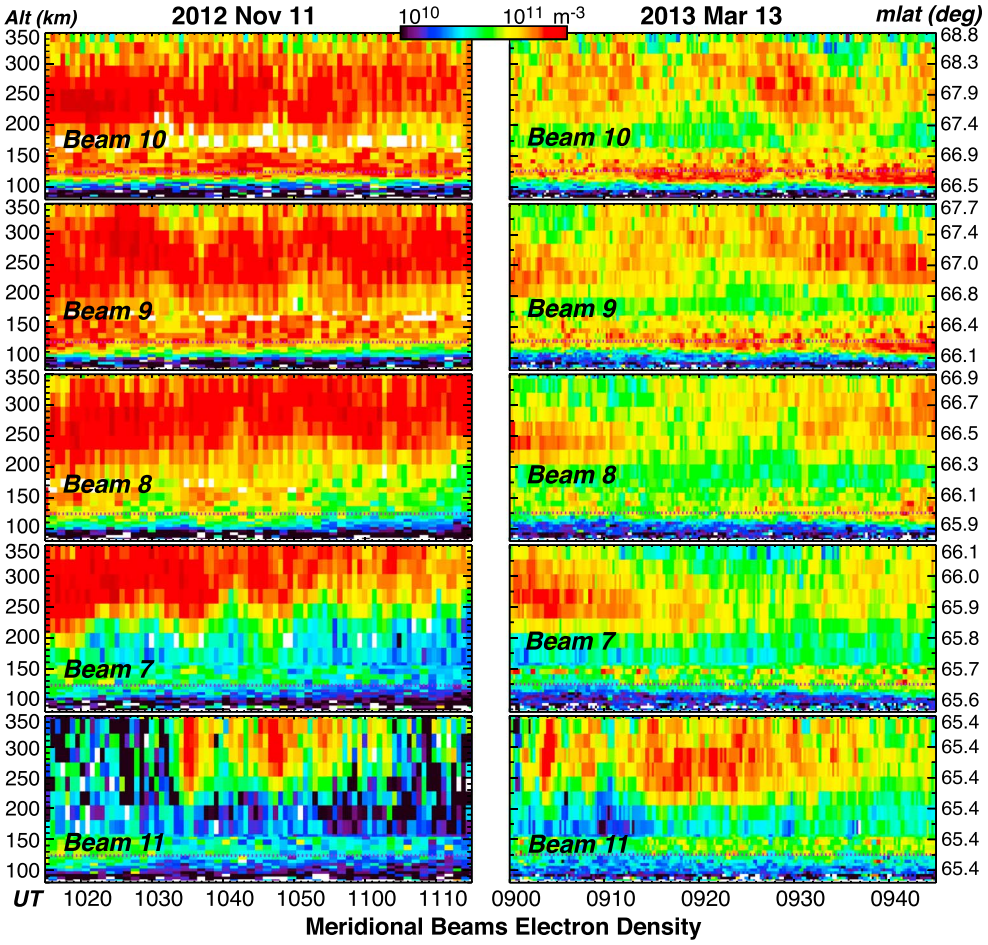

Figure 6. Electron densities measured by PFISR along all the central meridian beams, as well as along the up *B* beam, from 10:15 to 11:15 UT on 11 November 2012 and from 09:00 to 09:45 UT on 13 March 2013, which includes the times of the images in Figures 4 and 5. Densities below 150 km are shown from the alternating code transmission scheme, and densities above 150 km are shown from the long pulse. The dotted horizontal lines are drawn at 125 km to assist in identifying the ionization layer from proton precipitation.

Poker Flat ASI and PFISR. Snapshots for these two events are shown in Figure 7. For each event, the bottom row shows the PFISR LOS speed overlaid on the Poker ASI images at 3 times, while the top row shows the SuperDARN LOS speeds overlaid on the THEMIS ASI images at 3 times chosen to illustrate the same event. The PFISR LOS speeds are overlaid also in the top rows, allowing comparison of the two different spatial coverages. Movies of the full time sequence for the 7 March 2013 event are shown in Movies S4 and S5 in the supporting information for the SuperDARN-THEMIS ASI observations and the Poker ASI-PFISR observations, respectively. The approximate equatorward boundary of the diffuse equatorward auroral band is identified on each image with a short dashed line.

Westward moving auroral enhancements can be seen along the poleward edge of the diffuse aurora band for the 7 March 2013 as in earlier examples, although the oval is thinner for this event and auroral emissions are not seen poleward of these enhancements. The westward moving enhancements are particularly clear in Movie S4 in the supporting information, and corresponding flow enhancements seen by PFISR are identified in the figure. (The radar flows shown were processed with 60 s time resolution to reduce noise due to the large number of radar beams in the radar used on this day.) The THEMIS ASI images in the figure and in Movie S4 in the supporting information show that the westward moving auroral enhancements emanated from streamers within a thicker, bulge-like auroral oval to the west and outside the FOV of PFISR. Furthermore, the western looking SuperDARN beams

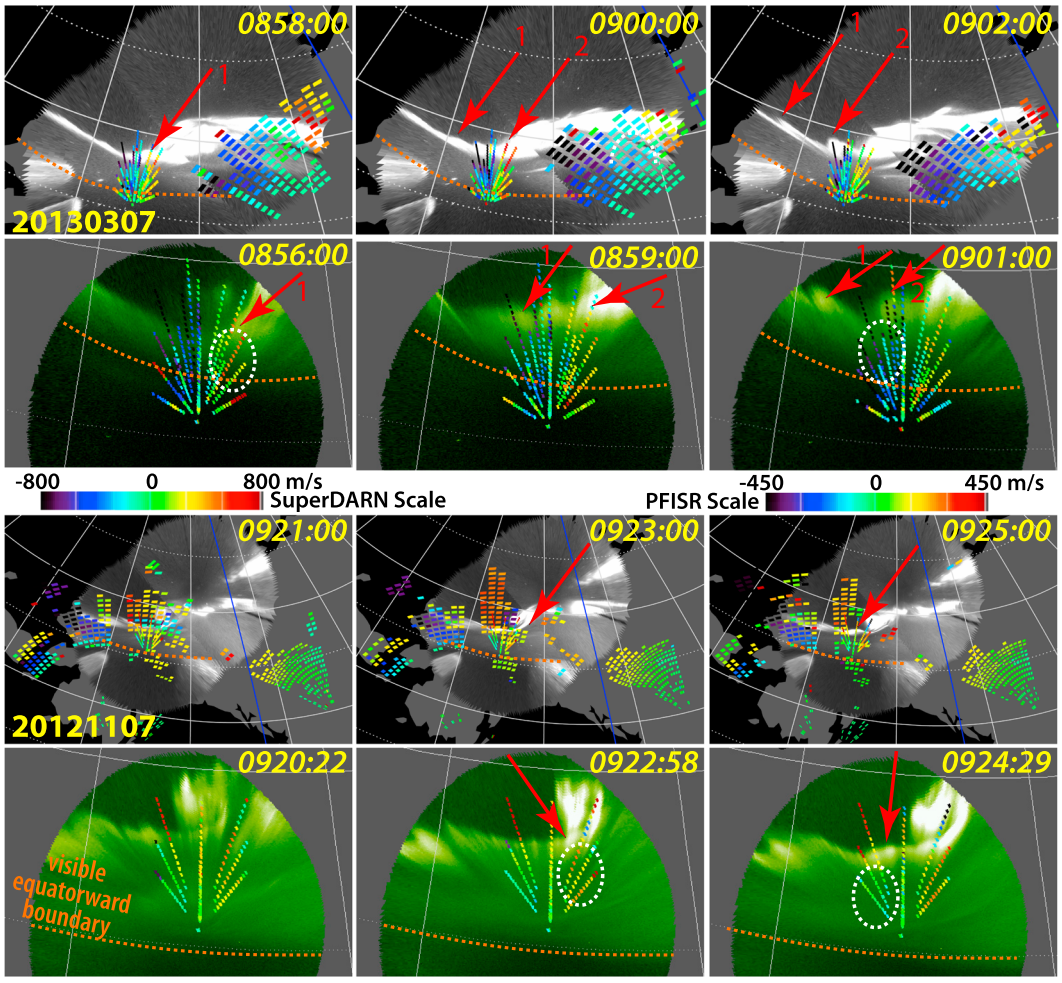

Figure 7. ASI and radar observations from events on (top row) 7 March 2013 and (bottom row) 7 November 2012 having good coverage from both neighboring THEMIS white-light ASIs and SuperDARN coherent-scatter radars. For each event, the bottom row shows PFISR LOS speed overlaid on the Poker ASI images at 3 times, and the top row shows the SuperDARN and PFISR LOS speeds overlaid on the THEMIS ASI images at 3 times chosen to illustrate the same event. The short dashed lines identify the equatorward boundary of the diffuse equatorward auroral band for each image.

show strong away from the radar flow speed of ~800 m/s approximately overlapping the equatorward diffuse auroral band in the region east of the PFISR FOV. The 7 November 2013 event shows similar features, except that the connection to streamers within bulge-like aurora was within the FOV of the POKER ASI, and the strong, westward SAPS flows were seen to the west of the PFISR FOV.

An interesting feature of these above two examples is that the azimuthal moving auroral enhancements (marked by red arrows) seen to the west of the bulge region were near the poleward of a relatively thin auroral oval but still connected to equatorward flows within a thicker oval to the east. Such a thin oval was seen for four of the six cases where azimuthally moving auroral enhancements were seen, but none were seen connecting to streamers. Thus, it is plausible that there was a connection to auroral streamers from a bulge region further to the east of the Poker ASI FOV, but either the event or good observing conditions ended well before the near-midnight MLT sector reached Poker Flat.

The two events here thus offer support for the possibility that the westward moving flow bursts that give the auroral enhancements generally form from earthward flow bursts within the plasma sheet and that these flow bursts can enter the SAPS that lies equatorward (earthward in the plasma sheet) of the electron auroral oval.

5. Conclusions

The examined ASI observations discussed here show that low-intensity, westward moving auroral enhancements are a common feature within and the near-diffuse auroral band that often lies equatorward of the main electron auroral oval. The radar data indicates that these auroral enhancements move together with bursts of enhanced westward flow lying adjacent to and just equatorward of the auroral enhancements. The diffuse auroral band is what is expected from proton precipitation from the partial ring current in the region equatorward of the auroral electron precipitation, and the electron densities measured by PFISR with this region show the thin lower *E* region density enhancement expected from proton precipitation. This corresponds to the expected region of SAPS, and the LOS velocities measured by PFISR are consistent with this being the region evidence of westward SAPS flows. The strong westward flows of SAPS within the apparent proton precipitation band have been further confirmed for the two of our events having broader radar echo coverage from SuperDARN over the diffuse precipitation band.

Our results indicate that while SAPS are often viewed as a region of relatively stable proton precipitation and westward flows, this may often not be the case. Instead, the region can consist of rapidly varying flows, with speeds varying from ~100 m/s to ~1 km/s in just a few minutes, the peaks appearing to be some of the flow enhancements that have been referred to as SAIDs. Based on our examples, the SAPS region also can include bursts of weak electron precipitation that move westward with the westward flow bursts and are visual seen in the aurora.

Additionally, our observations of streamers and associated LOS flows give evidence that the azimuthally moving flow bursts may often connect to earthward (equatorward in the ionosphere) plasma sheet flow bursts as illustrated by the red arrows in Figures 4 and 5. This would be consistent with previous case studies showing that some flow bursts turn azimuthally after reaching the inner plasma sheet and lead to the bursts of strong azimuthal flow. The cases presented here all show these flow bursts moving westward, suggesting a flow path that is guided by the duskside convection cell, flowing around the Harang reversal, and bring flows to the SAPS region. During four of our events, streamers were seen near the midnight sector and appearing to turn eastward. This suggests that there may be a general guiding by the large-scale convection pattern, where flow bursts within the duskside convection being azimuthal turned to the west and those within the dawn cell being turned toward the east.

As a concluding thought, we mention that coordinated observations with radars and ASIs have given evidence that plasma sheet flow bursts may be driven by enhanced equatorward flows that cross the poleward boundary of the auroral oval from the polar cap and enter the region of closed, plasma sheet field lines [*de la Beaujardière et al.*, 1994; *Pitkänen et al.*, 2013; *Shi et al.*, 2012; *Zou et al.*, 2014], and case studies using polar cap radars have provided evidence that such flows extend a considerable distance poleward of the nightside polar cap boundary [*Lyons et al.*, 2011; *Nishimura et al.*, 2010]. Furthermore, a recent study has given evidence that the flow enhancement within the polar cap might originate from localized dayside reconnection regions on the dayside [*Nishimura et al.*, 2014a]. It will thus be interesting to consider in the future whether the SAPS region flow structures considered here may be connected to flow enhancements that originate on the dayside, propagate across the polar cap, and then reach the nightside open-closed boundary, triggering localized nightside reconnection and flow bursts within the plasma sheet.

Acknowledgments

This work at UCLA was supported by National Science Foundation grants AGS1042255 and AGS1242356, NASA grant NNX13AD68G, and NASA contract NAS5-02099. The ASI data were supported by NSF grant AGS-1004736, and we thank the CSA for the logistical support in fielding and data retrieval from the THEMIS Ground-Based Observatory stations. SuperDARN is a collection of radars funded by national scientific funding agencies of Australia, Canada, China, France, Japan, South Africa, United Kingdom, and United States of America. J.M.R. acknowledges the support of NSF under award AGS-0946900. The Poker Flat Incoherent Scatter Radars is operated by SRI International on behalf of the U.S. National Science Foundation under NSF Cooperative Agreement AGS-1133009. The Poker Flat filtered ASI is operated in support of PFISR through a cooperative agreement with SRI and through a NASA O&M contract for Poker Flat sounding rocket support. Data of the THEMIS ASI and PFISR are publically available through http://themis.ssl.berkeley.edu and http://isr.sri.com/madrigal/. The Poker Flat ASI and SuperDARN data can be obtained from the PIs (D.L.H. and J.M.R.).

Michael Liemohn thanks Asgeir Brekke and Roderick Heelis for their assistance in evaluating this paper.

References

Angelopoulos, V., W. Baumjohann, C. F. Kennel, F. V. Coroniti, M. G. Kivelson, R. Pellat, R. J. Walker, H. Lühr, and G. Paschmann (1992), Bursty bulk flows in the inner central plasma sheet, *J. Geophys. Res.*, *97*(A4), 4027–4039, doi:10.1029/91JA02701.

Angelopoulos, V., et al. (1997), Magnetotail flow bursts: Association to global magnetospheric circulation, relationship to ionospheric activity and direct evidence for localization, *Geophys. Res. Lett.*, *24*(18), 2271–2274, doi:10.1029/97GL02355.

Birn, J., and M. Hesse (2013), The substorm current wedge in MHD simulations, *J. Geophys. Res. Space Physics*, *118*, 3364–3376, doi:10.1002/jgra.50187.

Birn, J., R. Nakamura, and M. Hesse (2013), On the propagation of blobs in the magnetotail: MHD simulations, *J. Geophys. Res. Space Physics*, *118*, 5497–5505, doi:10.1002/jgra.50521.

De la Beaujardière, O., L. R. Lyons, J. M. Ruohoniemi, E. Friis-Christensen, C. Danielsen, F. J. Rich, and P. T. Newell (1994), Quiet-time intensifications along the poleward auroral boundary near midnight, *J. Geophys. Res.*, *99*(A1), 287–298, doi:10.1029/93JA01947.

Donovan, E., et al. (2006), The THEMIS all-sky imaging array—System design and initial results from the prototype imager, *J. Atmos. Sol. Terr. Phys.*, *68*(13), 1472–1487, doi:10.1016/j.jastp.2005.03.027.

Donovan, E., E. Spanswick, J. Liang, J. Grant, B. Jackel, and M. Greffen (2012), Magnetospheric dynamics and the proton aurora, in *Auroral Phenomenology and Magnetospheric Processes: Earth And Other Planets*, edited by A. Keiling et al., pp. 365–378, AGU, Washington, D. C. [Available at http://onlinelibrary.wiley.com/doi/10.1029/2012GM001241/summary.]

Eather, R. H., and S. B. Mende (1972), Systematics in auroral energy spectra, *J. Geophys. Res.*, *77*(4), 660–673, doi:10.1029/JA077i004p00660.

Foster, J. C., and W. J. Burke (2002), SAPS: A new categorization for sub-auroral electric fields, *Eos Trans. AGU*, *83*(36), 393–394, doi:10.1029/2002EO000289.

Gallardo-Lacourt, B., Y. Nishimura, L. R. Lyons, S. Zou, V. Angelopoulos, E. Donovan, K. A. McWilliams, J. M. Ruohoniemi, and N. Nishitani (2014), Coordinated SuperDARN THEMIS ASI observations of mesoscale flow bursts associated with auroral streamers, *J. Geophys. Res. Space Physics*, *119*, 142–150, doi:10.1002/2013JA019245.

Gkioulidou, M., A. Ukhorskiy, D. G. Mitchell, T. Sotirelis, B. Mauk, and L. J. Lanzerotti (2014), The role of small-scale ion injections in the buildup of Earth's ring current pressure: Van Allen Probes observations of the March 17th, 2013 storm, *J. Geophys. Res. Space Physics*, *119*, 7327–7342, doi:10.1002/2014JA020096.

Henderson, M. G., G. D. Reeves, and J. S. Murphree (1998), Are north-south structures an ionospheric manifestation of bursty bulk flows?, *Geophys. Res. Lett.*, *25*, 3737.

Kauristie, K., V. A. Sergeev, T. I. Pulkkinen, R . J. Pellinen, V. Angelopoulos, and W. Baumjohann (1996), Study of the ionospheric signatures of the plasma sheet bubbles, in Third International Conference on Substorms 3 (ICS-3), p. 93, *Eur. Space Agency*, Noordwijk, Netherlands.

Kauristie, K., V. A. Sergeev, O. Amm, M. V. Kubyshkina, J. Jussila, E. Donovan, and K. Liou (2003), Bursty bulk flow intrusion to the inner plasma sheet as inferred from auroral observations, *J. Geophys. Res.*, *108*(A1), 1040, doi:10.1029/2002JA009371.

Lilensten, J., and M. Galand (1999), Proton-electron precipitation effects on the electron production and density above EISCAT (Tromsø) and ESR, *Ann. Geophys.*, *16*(10), 1299–1307, doi:10.1007/s00585-998-1299-8.

Lyons, L. R., T. Nagai, G. T. Blanchard, J. C. Samson, T. Yamamoto, T. Mukai, A. Nishida, and S. Kokubun (1999), Association between Geotail plasma flows and auroral poleward boundary intensifications observed by CANOPUS photometers, *J. Geophys. Res.*, *104*(A3), 4485–4500, doi:10.1029/1998JA900140.

Lyons, L. R., Y. Nishimura, H.-J. Kim, E. Donovan, V. Angelopoulos, G. Sofko, M. Nicolls, C. Heinselman, J. M. Ruohoniemi, and N. Nishitani (2011), Possible connection of polar cap flows to pre- and post-substorm onset PBIs and streamers, *J. Geophys. Res.*, *116*, A12225, doi:10.1029/2011JA016850.

Makarevich, R. A., A. C. Kellerman, J. C. Devlin, H. Ye, L. R. Lyons, and Y. Nishimura (2011), SAPS intensification during substorm recovery: A multi-instrument case study, *J. Geophys. Res.*, *116*, A11311, doi:10.1029/2011JA016916.

Mende, S. B., and R. H. Eather (1975), Spectroscopic determination of the characteristics of precipitating auroral particles, *J. Geophys. Res.*, *80*(22), 3211–3216, doi:10.1029/JA080i022p03211.

Mishin, E. V. (2013), Interaction of substorm injections with the subauroral geospace: 1. Multispacecraft observations of SAID, *J. Geophys. Res. Space Physics*, *118*, 5782–5796, doi:10.1002/jgra.50548.

Mishin, E. V., and W. J. Burke (2005), Stormtime coupling of the ring current, plasmasphere, and topside ionosphere: Electromagnetic and plasma disturbances, *J. Geophys. Res.*, *110*, A07209, doi:10.1029/2005JA011021.

Nakamura, R., T. Oguti, T. Yamamoto, and S. Kokubun (1993), Equatorward and poleward expansion of the auroras during auroral substorms, *J. Geophys. Res.*, *98*, 5743.

Nishimura, Y., et al. (2010), Preonset time sequence of auroral substorms: Coordinated observations by all-sky imagers, satellites, and radars, *J. Geophys. Res.*, *115*, A00I08, doi:10.1029/2010JA015832.

Nishimura, Y., et al. (2014a), Day-night coupling by a localized flow channel visualized by polar cap patch propagation, *Geophys. Res. Lett.*, *41*, 3701–3709, doi:10.1002/2014GL060301.

Nishimura, Y., J. Bortnik, W. Li, L. R. Lyons, E. F. Donovan, V. Angelopoulos, and S. B. Mende (2014b), Evolution of nightside subauroral proton aurora caused by transient plasma sheet flows, *J. Geophys. Res. Space Physics*, *119*, 5295–5304, doi:10.1002/2014JA020029.

Panov, E. V., M. V. Kubyshkina, R. Nakamura, W. Baumjohann, V. Angelopoulos, V. A. Sergeev, and A. A. Petrukovich (2013), Oscillatory flow braking in the magnetotail: THEMIS statistics, *Geophys. Res. Lett.*, *40*, 2505–2510, doi:10.1002/grl.50407.

Panov, E. V., W. Baumjohann, R. Nakamura, M. V. Kubyshkina, K.-H. Glassmeier, V. Angelopoulos, A. A. Petrukovich, and V. A. Sergeev (2014), Period and damping factor of Pi2 pulsations during oscillatory flow braking in the magnetotail, *J. Geophys. Res. Space Physics*, *119*, 4512–4520, doi:10.1002/2013JA019633.

Pitkänen, T., A. T. Aikio, O. Amm, K. Kauristie, H. Nilsson, and K. U. Kaila (2011), EISCAT-Cluster observations of quiet-time near-Earth magnetotail fast flows and their signatures in the ionosphere, *Ann. Geophys.*, *29*(2), 299–319, doi:10.5194/angeo-29-299-2011.

Pitkänen, T., A. T. Aikio, and L. Juusola (2013), Observations of polar cap flow channel and plasma sheet flow bursts during substorm expansion, *J. Geophys. Res. Space Physics*, *118*, 774–784, doi:10.1002/jgra.50119.

Rostoker, G., A. T. Y. Lui, C. D. Anger, and J. S. Murphree (1987), North-south structures in the midnight sector auroras as viewed by the VIKING imager, *Geophys. Res. Lett.*, *14*, 407.

Sergeev, V. A., O. A. Aulamo, R. J. Pellinen, M. K. Vallinkoski, T. Bösinger, C. A. Cattell, R. C. Elphic, and D. J. Williams (1990), Non-substorm transient injection events in the ionosphere and magnetosphere, *Planet. Space Sci.*, *38*(2), 231–239, doi:10.1016/0032-0633(90)90087-7.

Sergeev, V. A., et al. (2000), Multiple-spacecraft observation of a narrow transient plasma jet in the Earth's plasma sheet, *Geophys. Res. Lett.*, *27*(6), 851–854, doi:10.1029/1999GL010729.

Shi, Y., E. Zesta, L. R. Lyons, J. Yang, A. Boudouridis, Y. S. Ge, J. M. Ruohoniemi, and S. Mende (2012), Two-dimensional ionospheric flow pattern associated with auroral streamers, *J. Geophys. Res.*, *117*, A02208, doi:10.1029/2011JA017110.

Smirnova, N. V., A. N. Lyakhov, Y. I. Setzer, A. P. Osepian, C.-I. Meng, R. Smith, and H. C. Stenbaek-Nielsen (2004), Precipitating protons and their role in ionization of the polar ionosphere, *Cosm. Res.*, *42*(3), 210–218, doi:10.1023/B:COSM.0000033296.08433.94.

Spiro, R. W., R. A. Heelis, and W. B. Hanson (1979), Rapid subauroral ion drifts observed by Atmosphere Explorer C, *Geophys. Res. Lett.*, *6*(8), 657–660, doi:10.1029/GL006i008p00657.

Wolf, R. A., C. X. Chen, and F. R. Toffoletto (2012), Thin filament simulations for Earth's plasma sheet: Interchange oscillations, *J. Geophys. Res.*, *117*, A02215, doi:10.1029/2011JA016971.

Yeoman, T. K., and H. Lühr (1999), CUTLASS/IMAGE observations of high-latitude convection features during substorms, *Ann. Geophys.*, *15*(6), 692–702, doi:10.1007/s00585-997-0692-z.

Zesta, E., L. Lyons, and E. Donovan (2000), The auroral signature of earthward flow bursts observed in the magnetotail, *Geophys. Res. Lett.*, *27*(20), 3241–3244, doi:10.1029/2000GL000027.

Zesta, E., E. Donovan, L. Lyons, G. Enno, J. Murphree, and L. Cogger (2002), Two-dimensional structure of auroral poleward boundary intensifications, *J. Geophys. Res.*, *107*(A11), 1350, doi:10.1029/2001JA000260.

Zou, S., L. Lyons, M. Nicolls, and C. Heinselman (2009a), PFISR observations of strong azimuthal flow bursts in the ionosphere and their relation to nightside aurora, *Eos Trans. AGU*, *71*(6–7), 729–737, doi:10.1016/j.jastp.2008.06.015.

Zou, S., L. R. Lyons, M. J. Nicolls, C. J. Heinselman, and S. B. Mende (2009b), Nightside ionospheric electrodynamics associated with substorms: PFISR and THEMIS ASI observations, *J. Geophys. Res.*, *114*, A12301, doi:10.1029/2009JA014259.

Zou, Y., Y. Nishimura, L. R. Lyons, and E. F. Donovan (2012), A statistical study of the relative locations of electron and proton auroral boundaries inferred from meridian scanning photometer observations, *J. Geophys. Res.*, *117*, A06206, doi:10.1029/2011JA017357.

Zou, Y., Y. Nishimura, L. R. Lyons, E. F. Donovan, J. M. Ruohoniemi, N. Nishitani, and K. A. McWilliams (2014), Statistical relationships between enhanced polar cap flows and PBIs, *J. Geophys. Res. Space Physics*, *119*, 151–162, doi:10.1002/2013JA019269.